



13. ガス中を伝播する高強度レーザーパルスの自己組織化

Self-organization of high intensity laser pulses propagating in gases

James Koga

Advanced Photon Research Center, Japan Atomic Energy Research Institute

8-1 Umemidai, Kizu-chou, Souraku-gun, Kyoto-fu 619-0215

In recent years the development of high intensity short pulse lasers has opened up wide fields of science which had previously been difficult to study. Recent experiments of short pulse lasers propagating in air have shown that these laser pulses can propagate over very long distances (up to 12 km) with little or no distortion of the pulse. Here we present a model of this propagation using a modified version of the self-organized criticality model developed for sandpiles by Bak, Tang, and Weisenfeld. The additions to the sandpile model include the formation of plasma which acts as a threshold diffusion term and self-focusing by the nonlinear index of refraction which acts as a continuous inverse diffusion. Results of this simple model indicate that a strongly self-focusing laser pulse shows self-organized critical behavior.

Keywords: self-organization, high intensity laser pulse, neutral gas, plasma

1. Introduction

In recent years the development of ultrashort pulse high intensity lasers has made possible the study of a variety of phenomena which had previously not been possible. Of particular interest with regards to this paper are experiments where high intensity short pulse lasers have been observed to propagate over long distances in air^{1,2}. In one experiment a terawatt laser was observed to propagate over 12 km². Sophisticated computer simulations of the phenomenon of the propagation of high intensity laser pulses in air have been performed³. These simulations show that the pulse filaments and that the onset and recurrence of these filaments have features similar to strong turbulence in other physical systems³. In this paper we propose that this dynamic behavior of the self-focusing and filament formation of a high intensity beam is similar to a self-organized criticality (SOC)⁴. By using a model similar to that developed by Bak, Tang, and Weisenfeld (BTW)⁴ we show that some features of the self focusing beam system are reproduced and indicate characteristics similar to SOC.

2. Laser Pulse Propagation and Self-Organized Critical Behavior

When an intense laser beam propagates in a gas, there are three main processes which occur. One is the self-focusing of the beam due to the dependence of the index of refraction of the gas on the intensity of the laser⁵. The second is the formation of plasma due to the optical field ionization (OFI) of the gas by the laser⁶. When plasma forms, the laser light is defocused. The third process is the natural diffraction of the light which occurs due to the finite pulse size. These three processes compete with one another. If the laser pulse focuses too much, then plasma forms to stop the focusing of the pulse. Conversely, if too much plasma forms, then the pulse is defocused leading to the stop of plasma formation. The diffraction is continually occurring. It is the balance of these three processes, which can lead to stable filament formation of the laser pulse and resultingly a sustained channelling process⁷ (see Figure 1).

SOC which was introduced by BTW⁴ occurs throughout the natural world. Some SOC type systems include earthquakes, sunspot activity, lightning, and low frequency circuit noise. A SOC system usually has the following three characteristics: a slow driver, interaction domination, and a threshold value of some kind⁸.

In the propagation of intense laser pulses in neutral gases each of these characteristics are present. The slow driver is the self-focusing which occurs over nanosecond timescales and longer. The threshold value is the ionization threshold for OFI which occurs over very short timescales on the order of 10^{-15} seconds or shorter. The interaction domination is the formation of filaments which merge and disappear as the pulse propagates.

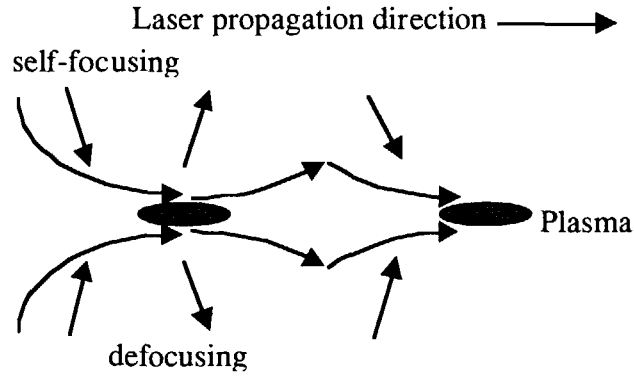


Fig. 1 Laser pulse propagation dynamics

3. Simulation Model

Each of the three processes mentioned above can be represented by a diffusion equation of the form

$$\frac{\partial Z}{\partial t} = D \frac{\partial^2 Z}{\partial y^2},$$

where Z is the amplitude of the laser pulse, y is the direction transverse to the propagation direction of the laser pulse, and D is the diffusion coefficient for each process. Finite differencing this equation we model the propagation of the intense laser pulse on a uniform 2 dimensional Cartesian grid. The amplitude $Z_{i,j}$ is taken to be the intensity of the laser at grid point (i,j) . The laser pulse is taken to be propagating along the x direction (i). OFI of the gas and, subsequently, the plasma formation by the laser occurs on very short time scales above the threshold intensity of the gas⁶. Therefore, we can model OFI as a step function-like process. When the amplitude $Z_{i,j} > Z_{crit}$, where Z_{crit} corresponds to the threshold intensity, plasma is created and the diffraction by the plasma is represented by

$$\begin{aligned} z_{i,j} &\rightarrow z_{i,j} - 2 \times D_p \times z_{i,j} \\ z_{i,j\pm 1} &\rightarrow z_{i,j\pm 1} + D_p \times z_{i,j} \end{aligned},$$

where the diffraction of the laser light occurs perpendicular to the propagation direction of the laser and D_p is the plasma diffusion coefficient,

$$D_p = \frac{c\Delta t}{n_0\Delta y} \theta_p$$

$$\theta_p = \sqrt{\frac{2\delta n}{n_0}} \quad \delta n = \frac{\omega_p^2}{2\omega_0^2}$$

where c is the speed of light, Δt is the timestep size, n_0 is the vacuum index of refraction, Δy is the grid size in the y direction, ω_p is the plasma frequency associated with the created plasma, and ω_0 is the laser frequency. This rule is executed across the grid until all values are less than or equal to Z_{crit} . This formulation is very similar to the one dimensional model of BTW⁴. In addition, since the created plasma remains, laser light behind the point where the plasma has formed is also diffracted using the same equation. In this model this is the only way that different parts of the laser beam communicate along the direction of propagation.

The self-focusing of the laser pulse due to the nonlinear polarization response of the gas is continually occurring and is represented by

$$z_{i,j} \rightarrow z_{i,j} + 2 \times \kappa \times z_{i,j}$$

$$z_{i,j\pm 1} \rightarrow z_{i,j\pm 1} - \kappa \times z_{i,j}$$

where the effect of the background gas focusing is linearly proportional to the intensity and κ represents the strength of the focusing,

$$\kappa = \frac{c\Delta t}{n_0\Delta y} \theta_f$$

$$\theta_f = \sqrt{\frac{2\delta n}{n_0}} \quad \delta n = n_2 I$$

where n_2 is the nonlinear index of refraction of the gas and I is the laser intensity.

Finally, the natural diffraction due to finite beam size is represented by

$$z_{i,j} \rightarrow z_{i,j} - 2 \times D \times z_{i,j}$$

$$z_{i,j\pm 1} \rightarrow z_{i,j\pm 1} + D \times z_{i,j}$$

where the diffraction of the laser light also occurs perpendicular to the propagation direction of the laser and D is the diffusion coefficient,

$$D = \frac{c\Delta t}{n_0\Delta y} \theta$$

$$\theta = \frac{0.61\lambda}{n_0 d}$$

where λ is the laser wavelength and d is the laser spot size. This natural diffraction is continually occurring.

4. Results

In Figure 2 a) we show the initial grid which is a 100x100 grid in the x and y directions, respectively.

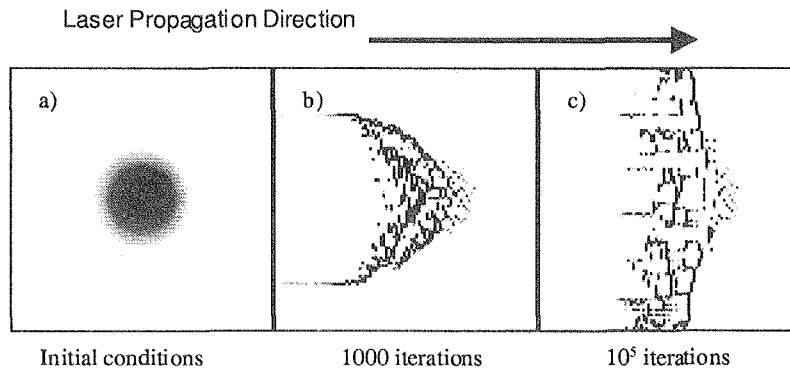


Fig. 2 a) Initial pulse, b) after 1000 iterations, and c) after 10^5 iterations

The initial configuration is a gaussian pulse with an initial maximum value of $Z_{max}=10$ with a sigma of 10 in both the x and y directions. The value of the plasma diffusion coefficient D_p was chosen to be 0.1 with $Z_{crit} = 12$. The value of κ was chosen to be 0.4 and the natural diffraction diffusion coefficient was chosen to be 0.1. κ was chosen larger than D otherwise the pulse would disperse too quickly and, resultingly, no ionizations would occur. This choice of parameters corresponds to a 14 GW laser pulse with a spot size of $100 \mu\text{m}$, and a time duration of 333 fs propagating in Xenon gas at atmospheric pressure over a distance of 15 m. In Figure 2 b) we show the result after the grid has been evolved for 10^3 iterations. It can be seen that filamentary structures have formed along the direction of propagation and that the pulse has broken up into many fragments. The front part of the pulse has narrowed and the back part of the pulse has filamented and widened. There are pockets behind the front of the pulse where no laser light is present. This is due to the fact that the plasma created at the front of the pulse has defocused the light behind. In Figure 2 c) after the pulse has evolved for 10^5 iterations the pulse has widened and the filament formation has moved forward in the pulse. This is due to the fact that the front of the pulse which has a lower intensity than the central peak takes a longer time to focus compared to the central part of the pulse. Thus, plasma creation occurs further forward in the pulse as the propagation continues. At each iteration the number of ionization events was recorded. Figure 3 shows the number of ionizations which occur as a function of iteration number. Initially there are no events, but as the pulse propagates the number of events increases. There is a peak which occurs in the number of ionizations very early on. This is attributed to the initial self-focusing of the laser pulse. After this point the number of ionizations saturates and appears to randomly fluctuate about a median value of about 1700.

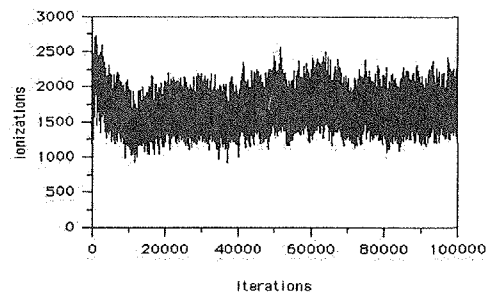


Fig. 3 Time series of ionizations

Figure 4 shows the power spectrum taken of the ionization time series. For low frequencies a clear power law can be seen. The fit to the low frequency spectrum gives an approximate power law of the form, $S(f) \sim 1/f$. At high frequencies the power law is flat indicating random noise.

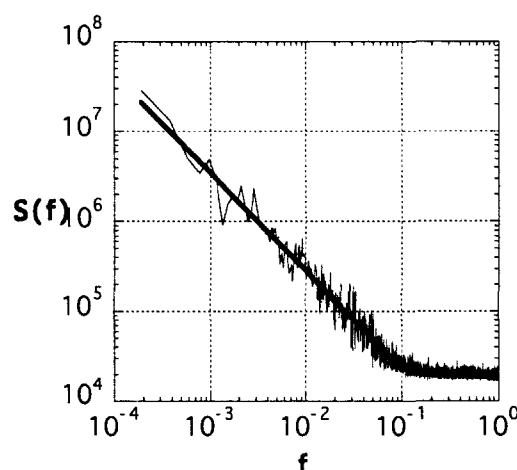


Fig. 4 Power spectrum of time series

The appearance of the $1/f$ type spectrum at low frequencies indicates that the ionizations occurring in the pulse are correlated over all timescales over which the power law occurs. We suggest that this correlation is brought about by the formation of plasma filaments at the front of the pulse which affect the formation of filaments in the back of the pulse. The random noise at high frequencies seems to correspond to the ionizations which are occurring in each filament. In animations of the evolution of the structures intermittent behavior in the formation of the filaments was observed. Intermittent structure formation is an indication towards SOC.

In simulations where the strength of the self-focusing is reduced sufficiently only a single filament forms over the propagation of the laser pulse. In this case the power spectrum of the ionization as a function of time also shows a power law behavior at low frequencies, but the power drops off steeper than $1/f$ and occurs over a smaller part of the spectrum. The high frequency flat spectrum occurs over more of the spectrum. At lower focusing strength with only one filament there are no other filaments to interact with and, therefore, correlations between the front and back of the pulse do not build up. The ionization is only occurring within the filament.

From these results is apparent that in order to get SOC type behavior one needs strong self-focusing and resultingly a large number of filaments forming.

5. Conclusion

We have developed a simple model for the propagation of intense laser pulses in neutral gases. The model is similar in aspects to the SOC model proposed by Bak, Tang, and Wiesenfeld⁴. The model differs from that model in that the discrete diffusion is performed in one direction. In the other direction the diffusion is chosen based on the position of previous threshold events. The model shows some behavior similar to that observed in more sophisticated simulations⁵ and shows intermittence and $1/f$ power law behavior in the ionizations induced by the laser which is a sign of possible SOC behavior. It appears that in order to get this SOC behavior strong self-focusing of the laser pulse is important. However, more detailed analysis is necessary. The next step will be to attempt to apply analytical theory such as Branching theory⁹ to laser pulse propagation and perform a parameter survey of the parameters relevant to experiments which have and will be performed with high intensity short pulse lasers.

References

- [1] A. Braun, G. Korn, X. Liu, D. Du, J. Squier, and G. Mourou, *Opt. Lett.* 20, 73 (1995).
- [2] L. Woste, C. Wedekind, H. Wille, P. Rairoux, B. Stein, S. Nikolov, C. Werner, S. Niedermeier, F. Ronneberger, H. Schillinger, and R. Sauerbrey, *Laser und Optoelectronik* 29, 52 (1997).
- [3] M. Mlejnek, M. Kolesik, J. V. Moloney, and E. M. Wright, *Phys. Rev. Lett.* 83, 2938 (1999).
- [4] P. Bak, C. Tang, and K. Wiesenfeld, *Phys. Rev. A* 38, 364 (1988).
- [5] R. W. Boyd, *Nonlinear Optics*, Academic Press, San Diego (1992).
- [6] L. D. Landau, E. M. Lifshitz, *Quantum Mechanics*, 3rd edn., Pergamon, London (1978).
- [7] A. Javan and P.L. Kelley, *IEEE Jour. of Quan. Elect.* QE-2, 470 (1966).
- [8] H. J. Jensen, *Self-Organized Criticality*, Cambridge University Press, Cambridge (1998).
- [9] T. E. Harris, *The Theory of Branching Processes*, Springer-Verlag, Berlin (1963).

14. 磁化プラズマ中の衝撃波による 超相対論的電子の生成

大澤幸治、 別所直樹
名古屋大学大学院理学研究科

Production of Ultrarelativistic Electrons by an Oblique Shock Wave in a Magnetized Plasma

Yukiharu OHSAWA, Naoki BESSHO

Department of Physics, Nagoya University, Nagoya 464-8602, Japan

Production of ultrarelativistic electrons in an oblique magnetosonic shock wave is studied with a one-dimensional, relativistic, electromagnetic, particle simulation code. It is found that a shock wave can accelerate some electrons to ultrarelativistic energies. Their Lorentz factors can exceed 100. The energies strongly depend on the shock angle.

Keywords : Particle acceleration, Ultrarelativistic electrons, Shock wave,
Particle simulation

1 背景と動機

宇宙では高エネルギーイオンだけでなく、高エネルギー電子もしばしば観測される。最近話題になったのは超新星残骸 SN1006 において電子が 10^{14} eV 程度に加速されているという報告である [1], [2]。Vela pulsar や Crab nebula においても電子が同程度のエネルギーにまで加速されているということである [3], [4]。これらの報告は、高エネルギー電子からのシンクロトロン放射による X 線、あるいは、逆コンプトン散乱によるガンマ線を観測することによってなされた。一方、太陽フレアに伴って高エネルギー電子が生成されることもよく知られている [5], [6]。太陽高エネルギー電子のエネルギーは数十 MeV 程度であり、加速に要する時間は非常に短く、数秒以下である。ここで、数秒というのは観測機器の時間分解能の最小単位であって、加速時間はそれより短いということである。このことは粒子加速モデルにとって非常に強い条件となる。

衝撃波によるイオン粒子の加速についての粒子シミュレーションは数多く報告されているが [7]-[14]、電子加速については今まで報告がなかった。ところが最近、磁場に対して斜めに伝播する衝撃波はロレンツ因子が 100 を超えるような超相対論的電子を生成することを、我々のグループが見出し、その物理的機構も明らかにした [15], [16]。

電子加速も含めた我々の一連の研究から、例えば以下のことが判る。(太陽磁力管のパラメータで) 磁気音波は 1. 陽子を短時間 (1 秒よりずっと短い時間) で相対論エネルギーにまで加速し、2. 全ての重イオンを同じスピードにまで加速し (従って、観測される重

イオンの組成は背景プラズマであるコロナの組成とほぼ等しい)、3. 100MeV 程度の電子を生成できる。これらは太陽高エネルギー粒子の基本的な性質である。つまり、太陽フレアが起こったとき、太陽磁力管の内部に大振幅の磁気音波が励起されると仮定すれば、太陽高エネルギー粒子の基本的な性質は説明できる。そして、フレアに伴って磁気音波を含めた様々な大振幅プラズマ波が励起されるという仮定は、フレアがあっても大振幅波が励起されないという（それ自身矛盾を含んだような）仮定よりもずっと自然である。

ここでは超相対論的電子の生成について報告する。第2節でシミュレーション結果を、第3節でまとめを述べる。詳細については文献 [15], [16] を参照していただきたい。

2 シミュレーション結果

シミュレーションは空間 1 次元、速度空間 3 次元の相対論的電磁粒子コードを用いて行った。このコードにおいては、電磁場は full Maxwell 方程式を解き、イオンと電子は相対論的方程式を解く。格子点の数が 4,096、シミュレーションにおける粒子数はイオンと電子それぞれが 26 万個ほどである。イオンと電子の質量比が 100、平衡状態における電子サイクロトロン周波数とプラズマ周波数の比は 3 ($\omega_{ce}/\omega_{pe} = 3$) である。図 1 に示すように、外部磁場が (x, z) 面内にあるプラズマ中を、 x 方向に磁気音波の衝撃波（パルス）が伝播する状況を考える。空間的变化は x 方向のみにあり、 y 方向、 z 方向には一様であるとする。衝撃波の伝播角度 θ は、外部磁場の x 成分を B_{x0} 、 z 成分を B_{z0} と置くと $\tan \theta = B_{z0}/B_{x0}$ で定義される。ただし、衝撃波中では磁場に y 成分も発生する。

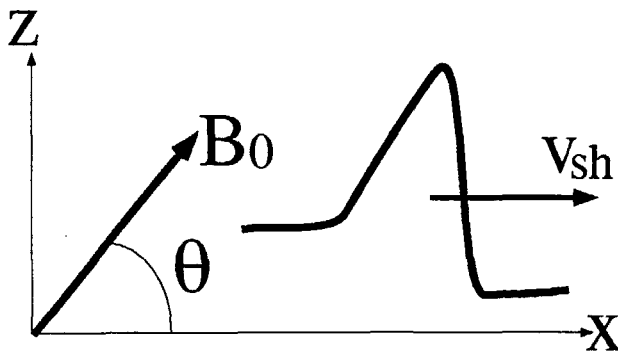


Fig. 1

図 1: 衝撃波と磁場の概念図

図 2 は、伝播角度 45 度、伝播速度がアルヴェン速度の 2.3 倍 ($v_{sh} = 2.3v_A$) の衝撃波における、ある瞬間の電子の位相空間図である。図の一点が位相空間における一つの電子の位置を表す。なお、 c/ω_{pe} は電子の skin depth である。上から順に、 (x, p_x) 、 (x, p_y) 、 (x, p_z) 、 (x, γ) 空間における図である。ここで、 p は粒子の運動量（図の表示は $m_e c$ で規格化されている）、 γ はロレンツ因子である。図から、 γ の値が 100 を超える電子が存在することが判る。最大の γ が存在する x 座標の位置は、磁場 B_z が（従って電位 φ が）最大

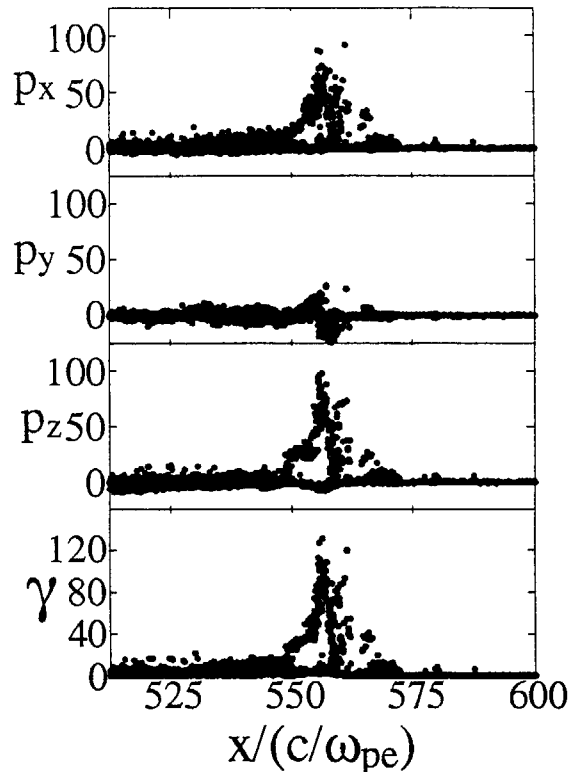


図 2: 電子の位相空間図

値をとる場所とほぼ一致している。

この加速の強さは衝撃波の伝播角度 θ に強く依存する。衝撃波速度 v_{sh} を一定にして、様々な伝播角度 θ の衝撃波をシミュレーションで調べてみた。そこで観測される電子の最大エネルギーを θ の関数として示したのが図3である。与えられたシミュレーション・パラメータに対して、理論は $\theta \sim 53^\circ$ で特に強い加速が起こることを予言するが、図3においてエネルギーが最大になるのは $\theta \sim 52^\circ$ であり、理論値と非常に近い。

3 終わりに

磁場に対して斜めに伝播する衝撃波は、高エネルギーイオンだけでなく、超相対論的エネルギーの電子を生成することができることを示した。もしも衝撃波パルスの後部で電子が反射されると、その電子はパルスに捕捉され、かつ、高エネルギーを持つようになる。ここで示した位相空間図では電子のエネルギーは $\gamma \sim 120$ であった。発表はしていないが、 $\gamma \sim 500$ 程度のシミュレーション結果もある。

加速される電子は殆ど捕捉領域から（すなわちパルス領域から）逃げ出さないで、パルス領域には徐々に捕捉電子の数が増えていく。これは宇宙のどこかで大振幅衝撃波が発生したときに、その波面近傍に超相対論的電子を生成し続け、なおかつそれらを捕捉し続けながら伝播する、ということで衝撃波面近傍がX線源、ガンマ線源となりうることを示唆している。このように捕捉粒子の数が増えていく場合、波がどのような影響を受けるか、大変興味がある。また、多次元のシミュレーションで捕捉粒子の逃げ出す機構（もしある

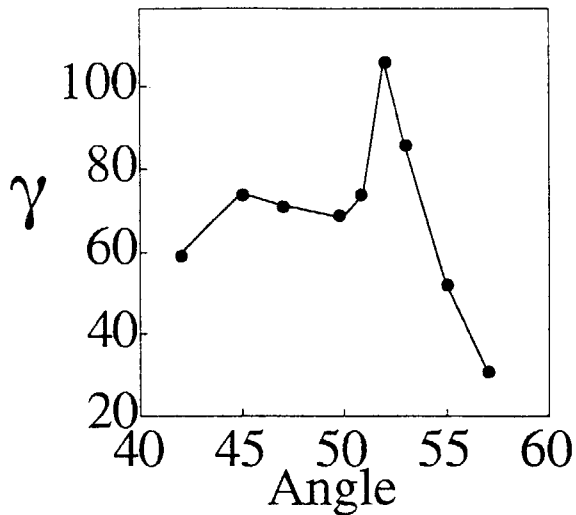


図 3: 最大電子エネルギーの伝播角に対する依存性

とすれば) を調べることも大事であろう。さらに、波の振幅を大きくしていけば、電子エネルギーもそれにつれて増大するか、ということは最も重要な課題である。

参考文献

- [1] K. Koyama, R. Petre, E. V. Gotthelf, *et al.*, *Nature* **378**, 255 (1995).
- [2] T. Tanimori, Y. Hayami, S. Kamei, *et al.*, *Astrophys. J.* **497**, L25 (1998).
- [3] T. Yoshimori, T. Kifune, S. A. Dazeley, *et al.*, *Astrophys. J.* **487**, L65 (1997).
- [4] T. Tanimori, K. Sakurazawa, S. A. Dazeley, *et al.*, *Astrophys. J.* **492**, L33 (1998).
- [5] S. R. Kane, K. Kai, T. Kosugi, S. Enome, P. B. Landecker, and D. L. McKenzie, *Astrophys. J.* **271**, 376 (1983).
- [6] S. R. Kane, E. L. Chupp, D. J. Forrest, G. H. Share, and E. Rieger, *Astrophys. J.* **300**, L95 (1986).
- [7] 大澤幸治, *日本物理学会誌* **45**, 637 (1990).
- [8] Y. Ohsawa, *J. Phys. Soc. Jpn.* **59**, 2782 (1990).
- [9] M. Toida, Y. Ohsawa, and T. Jyounouchi, *Phys. Plasmas* **2**, 3329 (1995).
- [10] M. Toida and Y. Ohsawa, *J. Phys. Soc. Jpn.* **64**, 2036 (1995).
- [11] M. Toida and Y. Ohsawa, *Solar Physics* **171**, 161 (1997).
- [12] D. Dogen, M. Toida, and Y. Ohsawa, *Phys. Plasmas* **5**, 1298 (1998).
- [13] K. Maruyama, N. Bessho, and Y. Ohsawa, *Phys. Plasmas* **5**, 3257 (1998).
- [14] T. Masaki, H. Hasegawa, and Y. Ohsawa, *Phys. Plasmas* **7**, 529 (2000).
- [15] N. Bessho and Y. Ohsawa, *Phys. Plasmas* **6**, 3076 (1999).
- [16] N. Bessho and Y. Ohsawa, *Phys. Plasmas* **7**, 4004 (2000).